SAND2011-7139C

DETERMINATION OF PRESSURE AND DENSITY OF SHOCKLESSLY COMPRESSED BERYLLIUM FROM X-RAY RADIOGRAPHY OF A MAGNETICALLY DRIVEN CYLINDRICAL LINER IMPLOSION

R. W. Lemke[1], M. R. Martin[1], R. D. McBride[1], J-P Davis[1], M. D. Knudson[1], D. B. Sinars[1], I. C. Smith[1], M. Savage[1], W. A. Stygar[1], K. Killebrew[2], D. G. Flicker[1], and M. C. Herrmann[1]

[1]Sandia National Laboratories, P.O. Box 5800, Albuquerque, New Mexico 87185, USA
[2]General Atomics, San Diego, California 92121, USA

Abstract. We describe a technique for measuring the pressure and density of a metallic solid, shocklessly compressed to multi-megabar pressure, through x-ray radiography of a magnetically driven, cylindrical liner implosion. Shockless compression of the liner produces material states that correspond approximately to the principal compression isentrope (quasi-isentrope). This technique is used to determine the principal quasi-isentrope of solid beryllium to a peak pressure of 2.4 Mbar from x-ray images of a high current (20 MA), fast (~100 ns) liner implosion.

Keywords: shockless compression, quasi-isentropic, liner, z-pinch, beryllium, radiography
PACS: 07.35.+k, 52.58.Lq, 64.30.Ef, 52.65.Kj

INTRODUCTION

Pulsed-power driven liner implosions can be used to produce extreme pressure states in condensed matter that are relevant to the study of planetary interiors, astrophysics, and inertial confinement fusion [1]. The Z accelerator [2,3] delivers a current pulse to a cylindrical liner (tubular shell) that rises to a peak of 20-26 MA in ~100 ns (depending on load inductance). The magnetic pressure on a cylindrical liner is proportional to I^2/R_o^2 , where I is the current at the outer radius R_o of the liner. For I=20 MA the magnetic pressure exceeds 28 Mbar on the liner surface for $R_o \leq 0.15$ cm, which is about a factor of 4 larger than can be produced in the planar platforms used for high pressure EOS (equation of state) studies on Z [4,5].

We discuss results of cylindrical, quasi-isentropic compression experiments on the Z accelerator in which x-ray radiography of a liner Z-pinch implosion is used to measure the density and pressure of shocklessly compressed, solid beryllium (Be) to a peak pressure of 2.4 Mbar.

In these experiments the magnetic pressure (field) is applied directly (direct drive) to the outer radius of a Be liner. The initial liner characteristics are inner radius 2.39 mm, outer radius (R_0) 3.19 mm, axial length 6.5 mm, density (ρ) 1.85 g/cm^3, and mass (M) 169 mg. This liner is fixed at one end to the cathode and at the other end to the anode; it is enclosed by a 13 mm radius, 0.125 mm thick, coaxial, Be tube that is part of the anode return current structure. Beryllium is used for the liner and

return current structure because this configuration is semi-transparent to the available monochromatic, 6151 eV backlighter source. This backlighter system is capable of producing two radiographs per Z shot with a time separation ranging from 2 ns to 20 ns and a spatial resolution of 15 μm [6].

The $\vec{J} \times \vec{B}$ force, where the current density $\vec{J}$ is axial and the magnetic field $\vec{B}$ is azimuthal, implodes the liner to its axis; multiple radiographs are taken at different times on its trajectory. Abel inversion, which assumes axial symmetry, is used to infer the liner density *ρ(r)* corresponding to each radiograph [7]. The liner density is given by

$$\rho(r) = \frac{1}{\pi\bar{\kappa}} \int_r^{R_0} \frac{dF}{dy} \frac{dy}{\sqrt{y^2 - r^2}}, \qquad (1)$$

where *y* is a coordinate in the image plane, $F(y) = I(y)/I_0$ is the normalized x-ray intensity at the image plane, $F(R_0) = 1$, and $\bar{\kappa}$ is the absorption opacity (in cm^2/g) of the Be liner. We assume that $\bar{\kappa}$ is unknown; the volume integral of the Abel inverted density profile must equal the known liner mass M, which determines a value for $\bar{\kappa}$.

Expressions for the total pressure $P_T(r,t)$ in the liner and the mass velocity $v(r,t)$ are derived using the hydrodynamic equations for conservation of mass and momentum in cylindrical coordinates. After transforming to the Lagrangian mass coordinate *m*, where $dm = 2\pi\rho r dr$, the governing equations can be written as

$$\frac{\partial(rv)}{\partial m} = \frac{1}{2\pi} \frac{D}{Dt}\left(\frac{1}{\rho}\right), \qquad (2)$$

$$\frac{\partial P_T}{\partial m} = -\frac{1}{2\pi r} \frac{Dv}{Dt}. \qquad (3)$$

where D/Dt represents $\partial/\partial t + v\,\partial/\partial r$.

Equations (2) and (3) are numerically integrated to obtain expressions for P_T and v as follows. Assume there are *N* radiographs in the range $t_1 \le t_n \le t_N$. Each Abel inverted density profile is divided into discrete bins of mass m_i^n, where $M = \sum_i m_i^n$. The *N* density profiles $\rho(r_i^n, m_i^n, t_n)$ are used to evaluate the right-hand-side (RHS) of Eq. (2), which is fit to a cubic spline and integrated to obtain a continuous function for $v(r,m,t)$. The latter is used to evaluate the RHS of Eq. (3), which is integrated to obtain a continuous function for the total pressure $P_T(r,m,t)$ over the temporal range of the radiographs. In the latter integration it is assumed that $P_T = 0$ on the inner surface of the liner. The total pressure P_T is the sum of the radial components of hydrodynamic and magnetic pressure, and possibly the radial component of deviatoric stress if strength effects are significant.

The rise time of the current pulse on Z is shaped to produce a dynamic drive pressure at the liner surface that compresses Be quasi-isentropically during the implosion [3-5]. The precise current wave form is based on the compression isentrope of Be; it is determined a priori by two-dimensional numerical simulation of the experiment using the ALEGRA radiation magneto hydrodynamics code [5,8]. Sesame table 2020 was used for the EOS of Be [9].

EXPERIMENTS AND RESULTS

The measured shaped currents used in these experiments are plotted in Fig. 1 for two identical shots on Z (2108 and 2110). Evidently, the shaped current is accurately produced in both shots. The vertical dashed lines define the temporal window for the multi-frame, x-ray radiography. The two shots yielded four radiographs in this window at times 3.035 and 3.050 μs in 2108, and 3.027 and 3.046 μs in 2110.

Also plotted in Fig. 1 are velocities of the inner liner surface as functions of time from ALEGRA

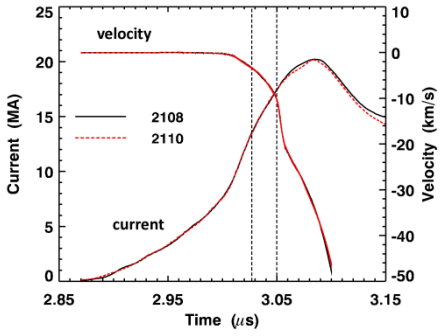

Figure 1. Measured currents from Z shots 2108 and 2110, and simulated liner velocities vs. time.

simulations driven by the measured currents. The velocities show no sign of shock-up; they are nearly identical for the two cases through the latest radiograph time. This indicates that the liners in the two shots experienced the same acceleration (pressure) history through this time. Hence, we conjecture that the magnetic pressure drive that compresses and implodes the liners is nearly identical in both shots, which is a key requirement of the technique, and we treat the four radiographs as if they were produced in a single shot.

The late time (3.050 μs) radiograph and corresponding z-averaged, normalized intensity versus radius are shown in Figs. 2(a) and 2(b), respectively. The vertical dashed lines in Fig. 2(a) indicate the original location of the liner; the 1 mm diameter black region centered on the axis is indicative of the tungsten rod used to quench self-emission during the liner implosion. The effect of random background noise, which produces uncertainty in the densities, is reduced by averaging the intensity in the z direction prior to performing the Abel inversions.

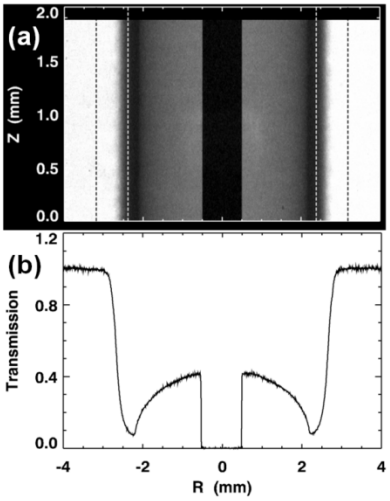

Figure 2. (a) Radiograph from Z shot 2108 at time 3.050 μs; white (black) is 100% transmission (absorption). (b) Average of radiograph intensity in z vs. radius.

Abel inverted liner densities corresponding to the four measured radiographs are plotted versus radius in Fig. 3; superimposed are densities at equivalent times from ALEGRA simulations that are indicative of shockless compression, which provides indirect proof that this was achieved in the experiment. The opacity of the Be liner deduced from the Abel inversions is in the range $2.25 \leq \bar{\kappa} \leq 2.61$ cm^2/g, with an average value of 2.42 ± 0.12 cm^2/g that is in good agreement with the value of 2.39 cm^2/g for solid Be and photon energy 6151 eV [10]. Error bars on the measured densities are determined by analysis of the propagation of uncertainty in the transmission intensity due to random noise, and uncertainty in $\bar{\kappa}$.

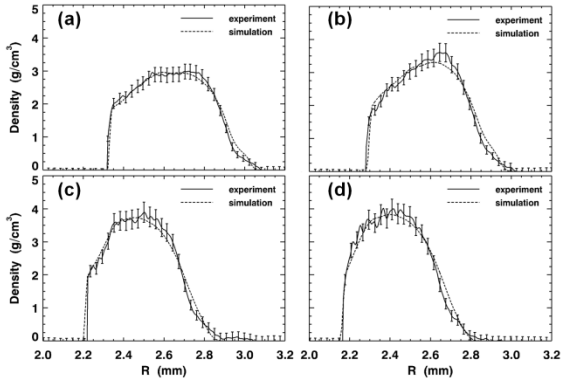

Figure 3. Abel inverted densities vs. radius from measured radiographs at times 3.027 μs (a), 3.035 μs (b), 3.046 μs (c), and 3.050 μs (d); superimposed on each plot is the corresponding simulated density.

The measured density profiles in Fig. 3 are used in Eqs. (2) and (3) to obtain the total pressure P_T. The measured P_T versus measured density is plotted in Fig. 4; superimposed is the compression isentrope of Sesame EOS 2020. The error bars are established by solving Eqs. (2) and (3) for random variations in the measured density and $\bar{\kappa}$ about their averages. The measured pressure is consistent with the Be 2020 isentrope up to a density (pressure) of 3.6 g/cm^3 (2.4 Mbar) where they diverge. The result in Fig. 4 is independent of, but consistent with, results of the ALEGRA simulations used to design the experiments, which used the Be 2020 EOS, and would appear to validate this EOS in the pressure range $0.3 \leq P_T \leq 2.4$ Mbar.

The results in Fig. 5 reveal that the measured P_T diverges from the Be 2020 isentrope in Fig. 4 where the magnetic pressure becomes significant relative to the hydro pressure. Plotted in Fig. 5

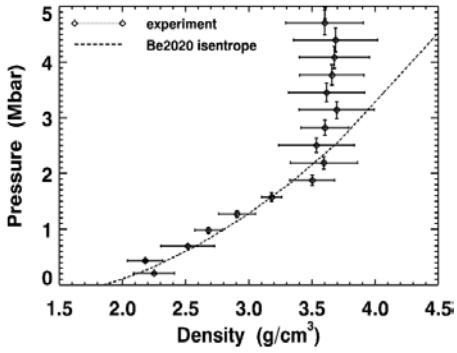

Figure 4. Measured pressure vs. density in beryllium.

versus radius at time 3.046 μs are the measured density and total pressure P_T, the corresponding simulated, z-averaged hydrodynamic and magnetic pressures (respectively P_H and P_B), density, and an integer quantity called phase that indicates whether the Be is solid (phase=1) or not (phase=3) as determined by a Lindeman melting law [11]. The simulated results show that 200 μm of Be is solid

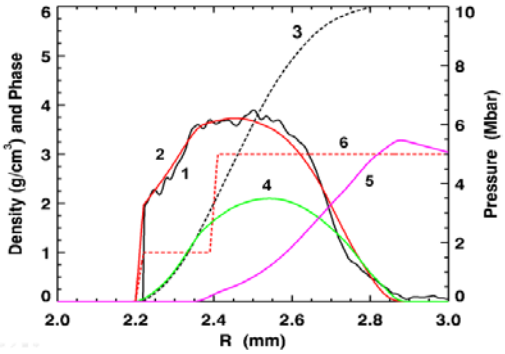

Figure 5. Abel inverted density (1) and measured total pressure P_T (3) vs. radius at time 3.046 μs; superimposed are the simulated density (2), hydro P_H (4) and magnetic P_B (5) pressures, and material phase (6).

(phase=1) at this time, and is quasi-isentropically compressed to a peak density and pressure of 3.6 g/cm^3 (compression ratio 1.9) and 2.4 Mbar, respectively. The fraction of the liner that is not solid is due solely to Joule heating associated with the magnetic field, which diffuses into the liner. Melting of compressed Be is well correlated with where the magnetic field exceeds 250 T; this is also where the hydro and magnetic pressures begin to diverge, for P > 2.4 Mbar, which is consistent with the measured result in Fig. 4.

The result in Fig. 4 demonstrates the feasibility of using the proposed analysis technique to determine the quasi-isentropic pressure and density of a metallic solid from a temporal series of x-ray radiographs of a magnetically driven, cylindrical liner implosion. The cylindrically convergent geometry significantly increases the pressure that can be produced in EOS experiments on the Z accelerator relative to the planar configurations presently used, albeit with less accuracy [4]. The available backlighter energy (6151 eV) at the Z facility limited the liner material to Be; we estimate this also limits the observable peak density (pressure) to 5 g/cm^3 (6 Mbar). With no restrictions on backlighter energy pressures in the tens of megabars can be investigated for a wide range of liner materials.

Sandia National Laboratories is a multi-program laboratory managed and operated by Sandia Corporation, a wholly owned subsidiary of Lockheed Martin Corporation, for the U.S. Department of Energy's National Nuclear Security Administration under contract DE-AC04-94AL85000.

REFERENCES

1. R. E. Reinovsky et al., IEEE Trans. Plasma Sci. **36**, 112 (2008).
2. M. K. Matzen et al., Phys. Plasmas **12**, 055503 (2005).
3. D. H. McDaniel et al., in *Dense Z-Pinches*, proceedings of the 5th International Conference, Albuquerque, NM, edited by J. Davis, C. Deeney, and N. R. Pereira (AIP, Melville, NY, 2002), p. 23.
4. J-P Davis et al., Phys. Plasmas **12**, 056310 (2005).
5. R. W. Lemke et al., Int. J. Impact Eng. **38**, 472 (2011)
6. G. R. Bennett et al., Rev. Sci. Instrum. **79**, 10E914 (2008).
7. C. J. Dasch, Appl. Opt. **31**, 1146 (1992).
8. A. C. Robinson et al., Comput. Phys. Commun. **164**, 408 (2004).
9. K. S. Holian, Los Alamos National Laboratory Report No. LA-10160-MS, 1984 (unpublished).
10. J. H. Hubbell and S. M. Seltzer, National Institute of Standards and Technology Report NISTIR 5632 (1995).
11. D. J. Steinberg et al., J. Appl. Phys. **51**, 1498 (1980).